symmetry

MDPI

Article

A Novel 2D—Grid of Scroll Chaotic Attractor Generated by CNN

Ahmed M. Ali *, Saif M. Ramadhan and Fadhil R. Tahir

Department of Electrical Engineering, University of Basrah, Basrah 61002, Iraq; saif.muneam@gmail.com (S.M.R.); fadhilrahma.creative@gmail.com (F.R.T.)
* Correspondence: ahmed.m.ojiemy@gmail.com; Tel.: +964-7822079703

Received: 1 December 2018; Accepted: 7 January 2019; Published: 16 January 2019

Abstract: The complex grid of scroll chaotic attractors that are generated through nonlinear electronic circuits have been raised considerably over the last decades. In this paper, it is shown that a subclass of Cellular Nonlinear Networks (CNNs) allows us to generate complex dynamics and chaos in symmetry pattern. A novel grid of scroll chaotic attractor, based on a new system, shows symmetry scrolls about the origin. Also, the equilibrium points are located in a manner such that the symmetry about the line $x = y$ has been achieved. The complex dynamics of system can be generated using CNNs, which in turn are derived from a CNN array (1×3) cells. The paper concerns on the design and implementation of 2×2 and 3×3 2D-grid of scroll via the CNN model. Theoretical analysis and numerical simulations of the derived model are included. The simulation results reveal that the grid of scroll attractors can be successfully reproduced using PSpice.

Keywords: chaos; Chua model; grid of scroll; CNN; nonlinear circuits

1. Introduction

Since the treasure trove of Chua's circuit [1], many scientists from different fields have been studying the double scroll attractors. Chua's circuit is a paradigm for chaos, which in turn is deformed from 3D system. Many bifurcation phenomena have been described in [2], such as Hopf bifurcation, Rossler's spiral, double scroll, etc., all these special emphases lead to the double scroll attractor. Leon O. Chua and Lui-nian Lin in [3], presented a canonical circuit capable of realizing every member of Chua's family using a three-region system. In [4], many strange attractors were found from Chua's oscillator and illustrated the complexity of Chua's oscillator. The implementation of a smooth nonlinearity with a cubic polynomial or higher order was presented in [5], to overcome some subtle features of a real circuit. In [6], Xiao Fan and Guanrong Chen designed a linear feedback controller composed with nonlinear modulo or sawtooth function to drive the original nonlinear autonomous system. Chen [7] introduced a canonical form of the generalized Lorenz system, which was deeply studied and found to be a new and useful tool for chaos synthesis. Moreover, Jinhu Lu and Guanrong Chen discovered a new chaotic system [8], that connects Lorenz attractor and Chen's attractor. A chaotic system of 3D quadratic smooth autonomous equations can generate two double-wing chaotic attractors [9]. A novel bounded 4D chaotic system was presented in [10], in which hyperchaos, chaos, equasiperiodic and periodic behavior were studied. In [11], Serdar et al. worked on numerical, electronic circuit simulation and electronic circuit implementation of a Sprott chaotic system and its synchronization.

For powerful ability in engineering applications based-chaos, chaotic attractors with high complex dynamic structures have been interestingly investigated. M. E. Ylcin et al. presented configuration of 3- and 5-scroll attractors from a generalized Chua's circuit that lead to n-scroll attractors [12]. In [13] (1D), (2D), and (3D) grid attractors the scroll generated due to equilibrium points. An approach proposed by Weihua Deng and Jinhu Lu in [14], generates multiscroll chaotic attractors including (1D) n-scroll,

(2D) $n \times m$-grid of scroll, and (3D) $n \times m \times l$-grid of scroll chaotic attractors. Jinhu Lu and Guanrong Chen survey the advantages of multiscroll chaotic attractors generation in potential applications and design theories [15]. Simin Yu et al. proposed a fourth-order double-tours circuit for creating (1D) n-tours, (2D) $n \times m$-tours, (3D) $n \times m \times l$-tours chaotic attractors [16]. In [17], a systematic threshold control approach for generating multi-scroll chaotic attractors was based on both general Jerk's and Chua's circuits with sine nonlinearity. In [18], a method was proposed for generating n-, $m \times n$-, and $m \times n \times l$-grid-scroll chaotic attractor based series of hyperbolic tangent function. In [19], generation of multiscroll $n \times m$-dimensional scroll was obtained from a one-dimension scroll by changing and adapting the system equation by jerk system. Zuo et al. used a CCII or current conveyor circuit for generating $4 \times 2 \times 2 \times 2$-scroll and $4 \times 2 \times 2 \times 2 \times 2$-scroll chaotic attractors which are basically fourth-order and fifth-order, respectively, via switching control [20]. Based on a general Jerk circuit, a new nonlinearity function for modulating and generating n-scroll chaotic attractors was proposed. This function is able to arbitrarily design the shapes, widths, swings, breakpoints, slopes, equilibrium points, and even the phase portrait of the n-scroll chaotic attractors and the chaos condition and dynamic mechanism of the jerk circuit are interestingly studied in [21]. A scheme is also designed for generating 3-scroll and 12-scroll chaotic attractors via switches and analog circuit realization. Simin Yu et al. suggested increasing the number of equilibrium points type index 2, by employing quadratic function, so they explored n- and $n \times m$-wing Lorenz attractors [22]. A sawtooth function can be used to generate multiscroll chaotic attractors by changing the number n of sawtooth function [23]. A simple circuit design was proposed in [24], capable of creating new grid multiscroll chaotic electronic oscillator. In [25], novel multiscroll attractors and multiwing hidden attractors in five dimensional memrestive system were proposed.

During the past two decades, different kinds of CNN-based chaotic circuits have facilitated the knowledge of the chaotic phenomenon by enhancing research on chaos through analog simulation. A 4D autonomous chaotic system was observed by introducing a state feedback and new n-well potential function for creating a butterfly wing chaotic attractor [26]. As a nonlinear circuit, CNN can be considered as a paradigm generator for complex systems [27]. Reasonable feedback from the states of the cells made the CNN-based chaotic circuit able to produce complex dynamics [28]. After developing the procedures of the CNN, great complex dynamic systems and chaotic circuits are modelled, such as Chua's circuit that was controlled by photoresistor nonlinear function [29]. Complex dynamics are proposed in [30] by fractional-order four-cell CNN, a system that exhibits high dynamical behavior such as periodic, chaotic and hyperchaotic. This dynamics behaviors are investigated numerically by simulations and theoretically by equations. A hyperbolic tangent function series is proposed in [31] to generate multi-scroll attractors such as 1D, 2D, and 3D scroll attractors from an autonomous SC-CNN system. Different approaches for simulating the multivariable nonlinearities by switching states of CNN in [32] based chaotic systems, Lorenz kind system dynamics and others like this one are generated by switching CNNs. In [33] it is shown that this structure, SC-CNN, is able to introduce complex dynamics, many circuits that exhibit complex dynamic behaviors can be obtained from this structure by changing the values of the cloning templates. On the other hand, CNN is a novel class of information-processing systems; like a neural network, it is a large-scale nonlinear analog circuit which processes signals in real-time. It was proposed and investigated by Chua and Yang in theory and applications [34,35]. In distinct cases, the CNN consists of a homogenous array and its array has no thresholds, no inputs, and even no outputs, and a sphere of influence that extends only to the nearest neighbours so the CNN reduces to a nonlinear lattice [36]. The local activity means that when the system exhibits complexity, the CNN parameters must be chosen so that the cells or their neighbours are locally actively coupled.

In this paper, a new model of CNN is presented using a modified Chua system. It is based on Piece Wise Linear (PWL) functions and the equilibrium points are distributed in such a way that give a symmetrical grid of scroll chaotic attractors. Next, to build CNN model scheme, we consider the generalized cell model that was introduced by Arena et al. [28]. The designed CNNs with array can

emulate such a system and generate a grid of scroll. The results showed that a grid of scrolls, 2×2 and 3×3, can be obtained using numerical simulations. The designed electronic circuit of a CNN model is also confirmed through the PSpice. The rest of paper is organized as follows. In Section 2, a new model for generation of a grid of scroll attractors is described. Its dynamical behavior is studied in Section 3. Section 4 covers a CNN based design to emulate the new system model and generation process of a grid of scroll using a CNN array. Section 5 describes the realization of a nonlinear electronics circuit and observation of a grid of scroll using PSpice. The conclusions are given finally.

2. The Generation of 2D-Grid of Scroll from a Modified Chua Model

The attention is to produce a complex chaotic attractor that has a grid of scrolls. The framework is the Chua chaotic oscillator model.

A. Chua Oscillator Model

The Chua oscillator model [37] is given by

$$\begin{aligned} \dot{x} &= \alpha[y - f(x)], \\ \dot{y} &= x - y + z, \\ \dot{z} &= -\beta y - \gamma z, \end{aligned} \tag{1}$$

$$f(x) = dx + \frac{1}{2}(c-d)[|x+1| - |x-1|], \tag{2}$$

Selecting parameters $\alpha = 9$, $\beta = 14.28$, $c = 1/7$, and $d = 2/7$, a typical double scroll Chua's attractor can be obtained, as shown in Figure 1. The equibilibrium points can be calculated as saddle index-2 $\left(\pm\frac{(\beta+\gamma)(d-c)}{\beta(d+1)+\gamma d}, \pm\frac{\gamma(d-c)}{\beta(d+1)+\gamma d}, \pm\frac{\beta(d-c)}{\beta(d+1)+\gamma d}\right)$ and saddle index-1 $(0,0,0)$. The double scrolls are evolving from index-2 equilibrium points as shown in Figure 1. Detailed studies of this model, its dynamics, and bifurcation can be found in [38].

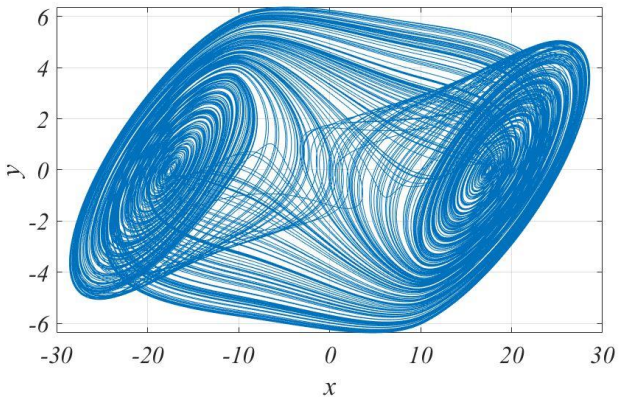

Figure 1. Double scroll attractor in the Chua oscillator chaotic model.

B. Modified Chua Oscillator Model

To create the 2D-grid of scroll chaotic attractors, it is essential to design a grid of saddle index-2 equilibrium points. System model (1) through (2), therefore, is developed to be

$$\begin{aligned} \dot{x} &= af(y) - bf(x), \\ \dot{y} &= x - y + z, \\ \dot{z} &= -\beta f(y), \end{aligned} \tag{3}$$

where a, b, and β are system parameters, suppose that $f(x)$ and $f(y)$ are PWL functions, which determine the number of scrolls in x and y directions, respectively. That is,

$$h(\xi_j) = m_{\xi_j\, q_{\xi_j}-1}\xi_j + \frac{1}{2}\sum_{i=1}^{q_{\xi_j}-1}\left(m_{\xi j\, i-1} - m_{\xi j\, i}\right)\left(\left|\xi_j + \xi_{ji}^b\right| - \left|\xi_j - \xi_{ji}^b\right|\right), \tag{4}$$

where $\xi_j \epsilon (x, y)$, $j \epsilon [1, 2]$, and $q_{\xi_j} (= 2, 3 \ldots)$ is the number of scrolls, $m_{\xi j\, i}$ and ξ_{ji}^b are the control parameters of PWL function. Figure 2 shows nonlinearity function.

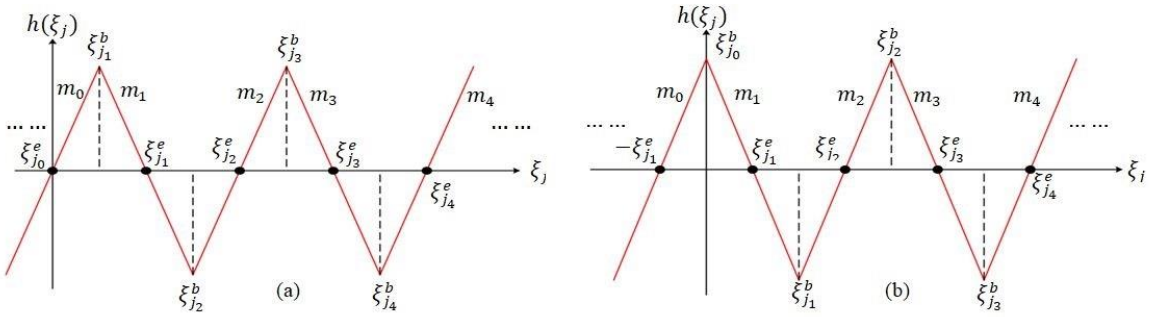

Figure 2. PWL function $h\left(\xi_j\right)$: (**a**) Odd number of scroll; (**b**) Even number of scroll.

C. Dynamics of New Model

Two essential features are focused on, the equilibrium points characteristics and bifurcation diagram to study the dynamics of the new model (3).

(*1*) *Equilibrium points:* As mentioned earlier, the distribution of saddle index-2 equilibrium points over the xy-plane to get a 2D grid of scroll chaotic attractor. By setting $\dot{x} = \dot{y} = \dot{z} = 0$, the equilibrium points can be discussed as follows:

- The equilibrium points $\pm y_i^e \left(i = 0, 1, 2, \ldots, q_{\xi_2} - 1\right)$ are located on the y-direction in the state space. One can deduce all positive equilibrium points by using the recursive formula which is given by

$$\begin{aligned} y_1^e &= \tfrac{\sum_{i=1}^{i}(m_k - m_{k-1})\xi_{2k}^b}{m_1}, \\ y_2^e &= \tfrac{\sum_{i=1}^{i}(m_k - m_{k-1})\xi_{2k}^b}{m_2}, \\ &\vdots \\ y_i^e &= \tfrac{\sum_{k=1}^{i}(m_k - m_{k-1})\xi_{2k}^b}{m_{q_{2-1}}}, \end{aligned} \tag{5}$$

- For the equilibrium points $\pm x_j^e \left(j = 0, 1, 2, \ldots, q_{\xi_1} - 1\right)$ which are located on the x-direction in the state space. The positive equilibrium points:

$$x_j^e = \left(\frac{a}{b}\right)\frac{\sum_{k=1}^{j}(m_k - m_{k-1})\xi_k^b}{m_{q_{1-1}}}, \tag{6}$$

- For the equilibrium points $\pm z_r^e = \left(r = 0, 1, 2, \ldots, \left(q_{\xi_1} - 1\right)\left(q_{\xi_2} - 1\right)\right)$ which are located on the z-direction in the state space. The positive equilibrium points:

$$z_r^e = y_i^e - x_j^e, i \in \left[0, 1, 2 \ldots . q_{\xi_2}\right],\ j \in \left[0, 1, 2 \ldots . q_{\xi_1}\right] \tag{7}$$

For example, when $q_{\xi_1} = q_{\xi_2} = 3$, a grid of 3×3 saddle index-2 equilibrium points can be obtained, as shown in Figure 3.

Obviously, system (3) with (4) has $(q_{\xi_1}-1)(q_{\xi_2}-1)$ equilibrium points. The corresponding jacobian matrices and their characteristic equations are, respectively,

$$J=\begin{bmatrix} -bm_{\xi_{1j}} & am_{\xi_{2i}} & 0 \\ 1 & -1 & 1 \\ 0 & -\beta m_{\xi_{2i}} & 0 \end{bmatrix} \tag{8}$$

and

$$\lambda^3+\lambda^2\left(1+bm_{\xi_{1j}}\right)+\lambda\left(bm_{\xi_{1j}}+\beta m_{\xi_{2i}}-am_{\xi_{2i}}\right)+\left(bm_{\xi_{1j}}\beta m_{\xi_{2i}}\right)=0 \tag{9}$$

Theoretical analysis shows that all equilibrium points can be classified into saddle index-2. For example, when $\beta=10$, a $=7$, $b=2.5$, $m_{\xi_{1o}}=1$, $m_{\xi_{11}}=-2$, $m_{\xi_{2o}}=2$, $m_{\xi_{21}}=-4$, and $q_{\xi j}=2$, system (3) with (4) has a 2x2-grid of equilibrium points. Similarly, for $\beta=10$, a $=7$, $b=2.5$, $m_{\xi_{1o}}=1$, $m_{\xi_{11}}=-2$, $m_{\xi_{2o}}=2$, $m_{\xi_{21}}=-4$, and $q_{\xi j}=3$, system (3) with (4) has a 3×3-grid of equilibrium points. Obviously, the equilibrium points have eigenvalues $\lambda_1=-4.3268$, $\lambda_{2,3}=0.4134\pm j3.531$ and $\lambda_1=-5.755$, $\lambda_{2,3}=4.877\pm j3.772$, which are called saddle points of index-2 since the two complex conjugate eigenvalues have positive real parts.

(2) *Bifurcation diagram:* To confirm the existence of chaos in the new system (3) with (4), assume that the case of $q_{\xi j}=3$. Then, $\beta\in[7,12]$. The bifurcation diagram of the parameter β of system (3) with (4) can be obtained as illustrated in Figure 4.

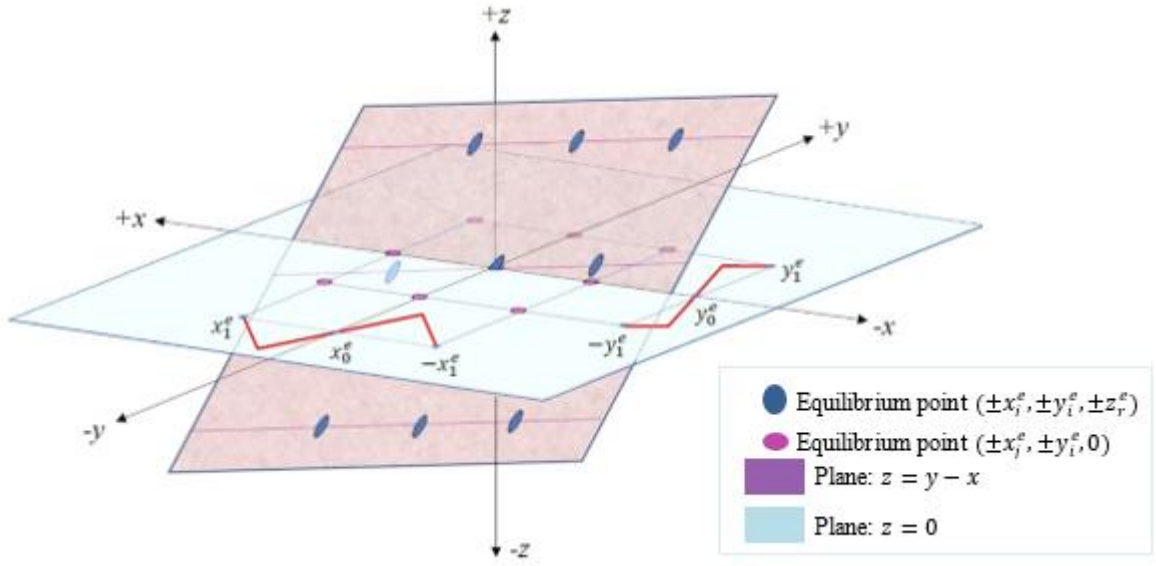

Figure 3. Grid of saddle index-2 equilibrium points, $q_{\xi_1}=q_{\xi_2}=3$.

D. Numerical Simulation Results

As mentioned in Section 2-C, there are $(q_{\xi_1}-1)(q_{\xi_2}-1)$ saddle index-2 equilibrium points. Considering the system parameters given in Section 2-C, a different 2D-grid of scroll chaotic attractors can be generated, as shown in Figure 5.

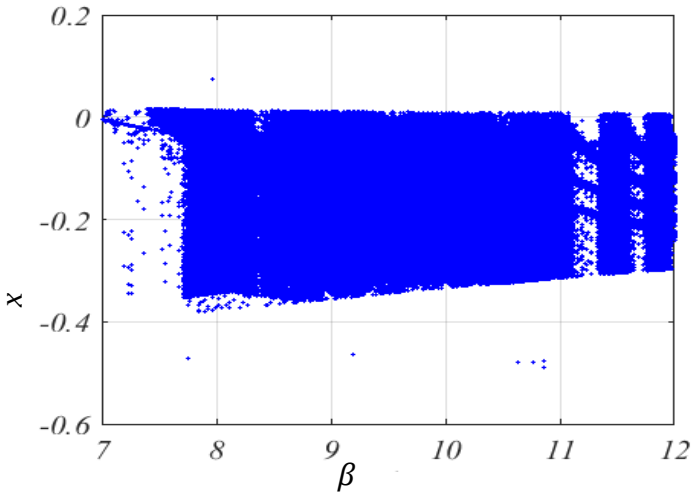

Figure 4. Bifurcation diagram of parameter β.

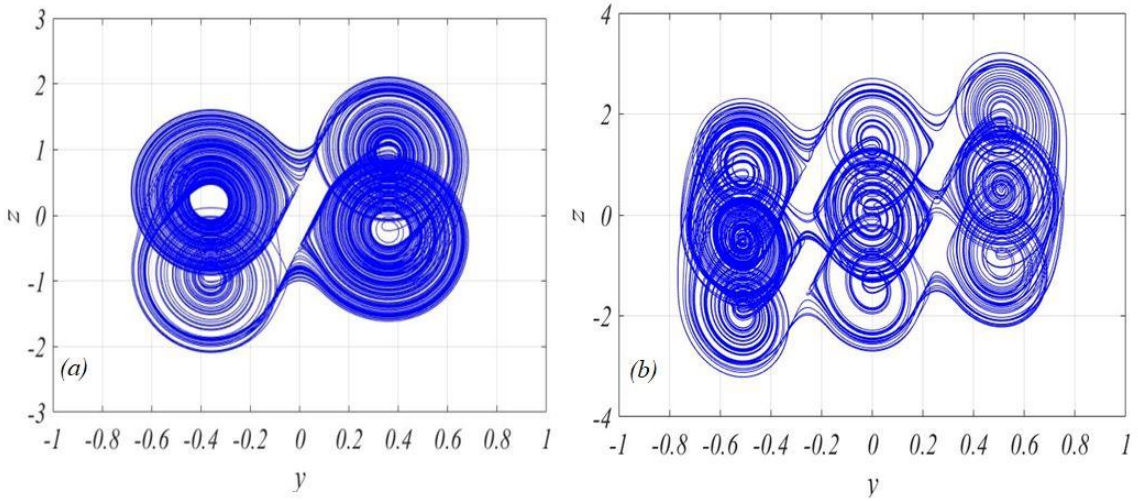

Figure 5. 2D-grid of scroll chaotic attractor on yz-plane. (**a**) 2×2 grid (**b**) 3×3 grid.

3. Design of CNN—Based New Chaotic System

This section introduces the design of chaotic system (3) with (4) based on CNN paradigm. A CNN can produce different forms of complex phenomena just like pattern formation, chaotic scroll, spiral, and autowaves. It works well as a merged model for complexity and a paradigm for simulating nonlinear partial differential equations (PDE's). Arena et al. [28] introduced the generalized cell model which is characterised by the following state equation:

$$\dot{x}_j = -x_j + a_j y_j + G_o + G_s + i_j, \tag{10}$$

with

$$y_j = \frac{1}{2}\left(|x_j + 1| - |x_j - 1|\right), \tag{11}$$

where x_j is the single state variable of cell, y_j is the single output state of cell, a_j, G_o, G_s, and i_j are parameters defining the CNN template. It is worth noting that the dynamics of state variables of the

single cell depend also on the state variables of neighbouring cells. According to model (10) with (11), the dynamic model of three fully connected CNN cells is

$$\begin{aligned} \dot{x}_1 &= -x_1 + a_1 y_1 + a_{12} y_2 + a_{13} y_3 + \sum_{k=1}^{3} s_{1k} x_k + i_1, \\ \dot{x}_2 &= -x_2 + a_{21} y_1 + a_{22} y_2 + a_{23} y_3 + \sum_{k=1}^{3} s_{2k} x_k + i_2, \\ \dot{x}_3 &= -x_3 + a_{31} y_1 + a_{32} y_2 + a_3 y_3 + \sum_{k=1}^{3} s_{3k} x_k + i_3, \end{aligned} \tag{12}$$

where x_1, x_2, and x_3 are state variables, y_1, y_2, and y_3 are the corresponding output. By choosing

$$a_{13} = a_{21} = a_{22} = a_{23} = a_{31} = a_{31} = a_{33} = 0;\ s_{13} = s_{22} = s_{33} = 0;\ i_1 = i_2 = i_3 = 0 \tag{13}$$

model (12) becomes:

$$\begin{aligned} \dot{x}_1 &= -x_1 + a_1 y_1 + a_{12} y_2 + s_{11} x_1 + s_{12} x_2, \\ \dot{x}_2 &= -x_2 + s_{21} x_1 + s_{23} x_3, \\ \dot{x}_3 &= -x_3 + a_{32} y_2 + s_{32} x_2 + s_{33} x_3, \end{aligned} \tag{14}$$

The new chaotic system (3) with (4) can be designed by CNN model to produce a 2D-grid of scroll chaotic attractor. So, two different paradigm layouts for generation of $n \times m$ 2D-grid of scroll chaotic attractor by CNN cells are adopted with different CNN cell parameters values, as shown in Table 1.

The design scheme of CNN cells connection is proposed for realizing model (14) as shown in Figure 6. Assuming that $V_1 = -Y_1$ and $V_2 = Y_2$ and $V_3 = X_2$ for the first cell, $V_1 = X_1$ and $V_2 = X_3$ for the second cell, $V_1 = -X_2$ and $V_2 = -Y_2$ for the third cell.

Table 1. Parameters of the designed Cellular Nonlinear Networks (CNN) model.

Grid \ Parameters	a_1	a_{12}	a_{32}	s_{11}	s_{12}	s_{21}	s_{23}	s_{32}	s_{33}
2×2-scroll	15.0	−25.2	36.0	−1.5	7.0	1.0	1.0	−10.0	1.0
3×3-scroll	−7.5	46.2	−66.0	−1.625	15.4	1.0	1.0	−22.0	1.0

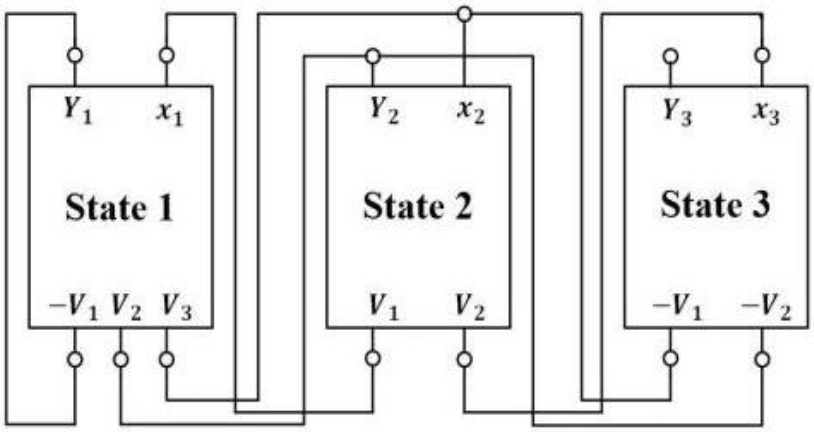

Figure 6. Scheme of fully interconnected CNN with three cells.

4. CNN Circuit Implementation

In CNN-based implementations, a state variable of the system to be realized is the voltage across capacitor of the Op-Amp based circuit design which is used to implement the dynamics of a CNN cell.

A circuit scheme for CNN model is proposed as shown in Figure 7 and it is govering by the following state equations:

$$\begin{aligned} \frac{dX_1}{dt} &= \frac{1}{R_6C_1}\left(\frac{R_5}{R_2}Y_1 + \frac{R_5}{R_3}Y_2 + \frac{R_5}{R_4}X_1 + \frac{R_5}{R_1}X_2\right), \\ \frac{dX_2}{dt} &= \frac{1}{R_{11}C_2}\left(\frac{R_9}{R_7}X_1 - X_2 + \frac{R_9}{R_8}X_3\right), \\ \frac{dX_3}{dt} &= \frac{1}{R_{15}C_3}\left(\frac{R_{14}}{R_{12}}Y_2 + \frac{R_{14}}{R_{11}}X_2\right), \end{aligned} \tag{15}$$

It is mainly constructed by six blocks, which are as follows:

i. N_1 is the first state variable generator; $a_1 = \frac{R_5}{R_3}$, $a_{12} = \frac{R_5}{R_2}$, $s_{11} = \frac{R_5}{R_4}$, $s_{12} = \frac{R_5}{R_1}$.

ii. N_2 is the second state variable generator; $s_{23} = \frac{R_{10}}{R_8}$, $s_{21} = \frac{R_{10}}{R_7}$.

iii. N_3 is the third state variable generator; $a_{32} = \frac{R_{14}}{R_{13}}$, $s_{32} = \frac{R_{14}}{R_{12}}$.

iv. N_4 is an inverting amplifier block with unity gain.

v. Both Y_1 and Y_2 are the nonlinearities of the CNN.

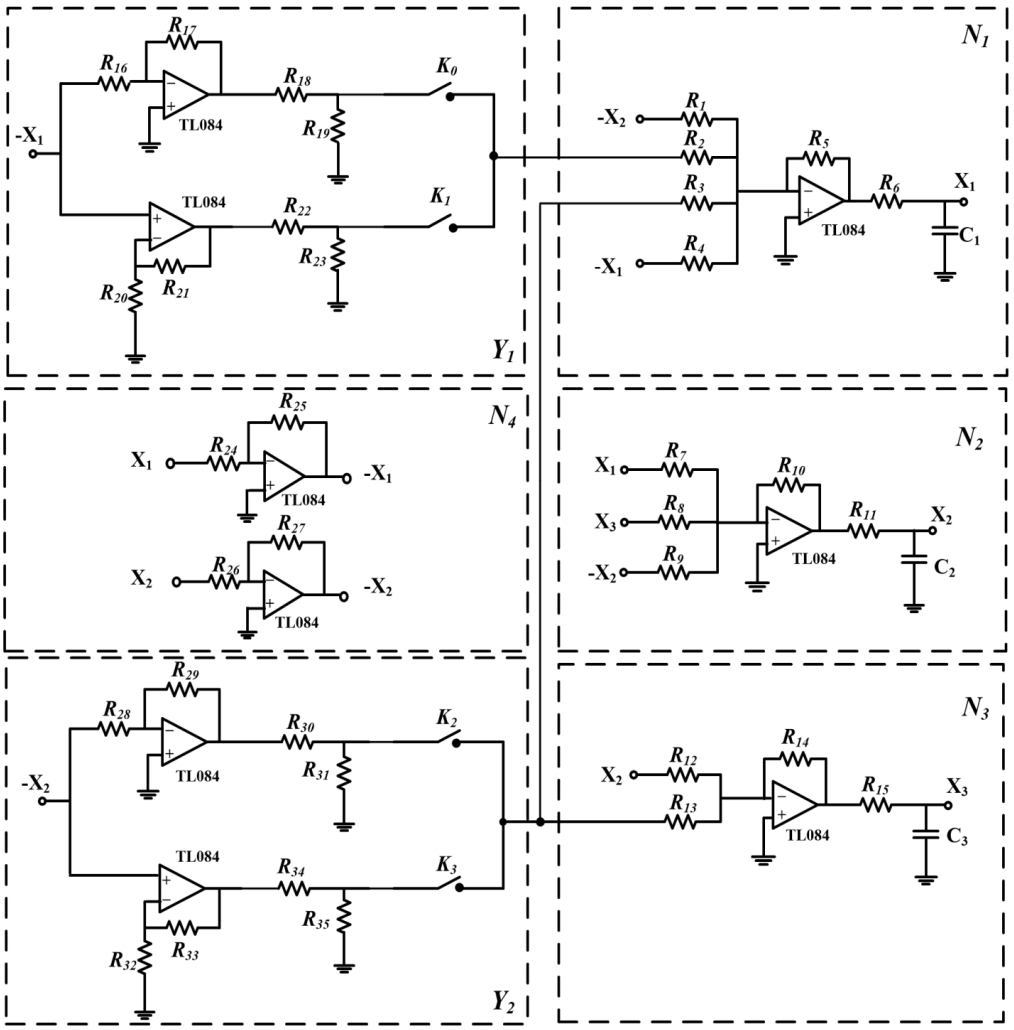

Figure 7. The CNN circuit scheme of system (13). The components are chosen as follows: $R_1 = 0.1428\ k\Omega$, $R_2 = 0.066\ k\Omega$, $R_3 = 0.00396\ k\Omega$, $R_4 = 0.4\ k\Omega$, $R_5 = R_7 = R_8 = R_9 = R_{18} = R_{19} = R_{20} = R_{22} = R_{23} = R_{24} = R_{25} = R_{26} = R_{27} = R_{30} = R_{31} = R_{32} = R_{34} = R_{35} = 1\ k\Omega$, $R_6 = 10\ k\Omega$, $R_{11} = 8\ k\Omega$, $R_{12} = 0.1\ k\Omega$, $R_{13} = 0.027778\ k\Omega$, $R_{14} = 1\ k\Omega$, $R_{15} = 5\ k\Omega$, $R_{16} = R_{28} = 10\ k\Omega$, $R_{17} = R_{29} = 1000\ k\Omega$, $R_{21} = R_{33} = 199\ k\Omega$, $C_1 = C_2 = C_3 = 100\ nF$.

The design of electronic circuit is based on capacitors, resistors, Op-Amps (TL084) of voltage supply equal to $\pm 12\ V$. The nonlinearities functions, Y_1 and Y_2, are implemented by using the circuitry block in such a different way so that it can be adapted by state of linkage switches. In accordance with the switches states that shown in Table 2, one can get different grids of scroll chaotic attractors. The PSpice simulations show that the new system (3) mutates to a CNN-based chaotic system and for selected values of the parameters. It shows chaotic dynamical behavior. The phase portraits are shown in Figure 8, on X_3X_2-plane projection.

Table 2. The $ON - OFF$ switch linkages $K_0 - K_3$.

Grids \ Switch	K_0	K_1	K_2	K_3
2×2-scroll	*ON*	*OFF*	*ON*	*OFF*
3×3-scroll	*ON*	*ON*	*ON*	*ON*

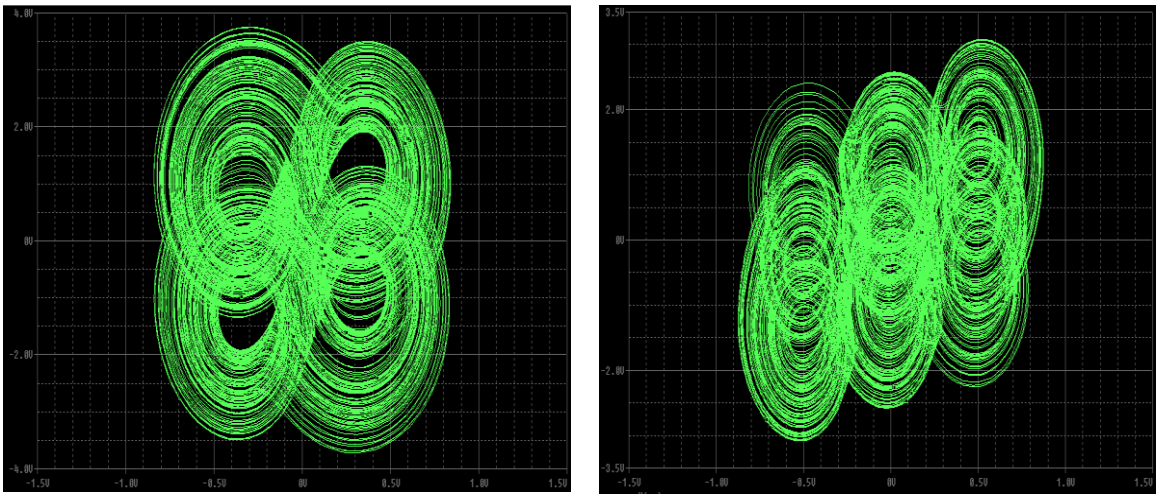

(**a**) (**b**)

Figure 8. PSpice results. Phase portraits of $n \times m$ grid scroll attractors of CNN circuit as: (**a**) 2×2; (**b**) 3×3 on X_3X_2-projection, $x = 0.5$ V/div, $y = 2$ V/div.

5. Conclusions

We have presented a novel third-order chaotic system and its complex dynamics. The new system is constructed by introducing two PWL functions that enable us to create a 2D-grid of scroll chaotic attractors. Such PWL function can be implemented by CNN model because its main block corresponds to saturation function. Dynamical analysis has been investigated, including equilibrium points and bifurcation. The equilibrium points distribution confirms the principle of symmetry. The locus y = x is the line of symmetry.

It can be noticed that this is the first CNN model reported in the literature that generates a 2D-grid of scroll chaotic attractor. Two different layouts generate a 2D-grid of scroll chaotic attractors by CNN cells. According to the selected parameters, a 2×2-scroll and a 3×3-scroll are confirmed. The system was implemented by using CNN cells. The PSpice environment results of the CNN model circuit design have demonstrated a good agreement with simulation results of the systems. The new system can be used in engineering applications based on chaos due to its capability of producing a grid of scroll attractors with a CNN circuitry.

Author Contributions: Methodology, A.-M.A.; Software, S.-M.R.; Supervision, F.-R.T.

Funding: This research received no external funding.

Conflicts of Interest: The authors declare no conflicts of interest.

References

1. Chua, L.; Komuro, M.; Matsumoto, T. The double scroll family: Part I: Rigorous Proof of chaos. *IEEE Trans. Circuits Syst.* **1986**, *33*, 1072–1118. [CrossRef]
2. Matsumoto, T.; Chua, L.O.; Komuro, M. Birth and death of the double scroll. *Phys. D Nonlinear Phenomena* **1987**, *24*, 97–124. [CrossRef]
3. Transaction, I.; Circuits, O.N. Canonical Realization of Chua's. *IEEE Trans. Circuits Syst.* **1990**, *37*, 885–902.
4. Chua, L.O.; Wu, C.W.; Huang, A.S.; Zhon, G.Q. A Universal Circuit for Studying and Generating Chaos 2. Strange Attractors. *IEEE Trans. Circuits Syst. I Fundam. Theory Appl.* **1993**, *40*, 745–761. [CrossRef]
5. Zhong, G. Implementation of Chua's Circuit with a Cubic Nonlinearity. *IEEE Trans. Circuits Syst. I Fundam. Theory Appl.* **1994**, *41*, 934–941. [CrossRef]
6. Wang, X.F.; Chen, G. Chaotification via arbitrarily small feedback controls: Theory, method, and applications. *Int. J. Bifurcation Chaos* **2000**, *10*, 549–570. [CrossRef]
7. Chen, G. On a generalized Lorenze canonical form of chaotic systems. *Int. J. Bifurc. Chaos Appl. Sci. Eng.* **2002**, *12*, 1789–1812.
8. Kong, H. A new chaotic attractor coined. *Int. J. Bifurc. Chaos* **2002**, *12*, 659–661.
9. Wang, L. Yet another 3D quadratic autonomous system generating three-wing and four-wing chaotic attractors. *Chaos* **2014**, *19*, 013107. [CrossRef]
10. Zhang, J.; Tang, W. A novel bounded 4D chaotic system. *Nonlinear Dyn.* **2012**, *67*, 2455–2465. [CrossRef]
11. Cicek, S.; UYAROĞLU, Y.; Pehlivan, I. Simulation and circuit implementation of sprott case H chaotic system and its synchronization application for secure communication systems. *J. Circuits Syst. Comput.* **2013**, *22*, 1350022. [CrossRef]
12. Suykens, J.A.K.; Vandewalle, J. Experimental Confirmation of 3- and 5-Scroll Attractors from a Generalized Chua's Circuit. *IEEE Trans. Circuits Syst. I Fundam. Theory Appl.* **2000**, *47*, 425–429.
13. Ozo, S. Families of scroll grid attractors. *Int. J. Bifurc. Chaos* **2002**, *12*, 23–41.
14. Deng, W. Design of multidirectional multiscroll chaotic attractors based on fractional differential systems via switching control. *Chaos* **2006**, *16*, 043120. [CrossRef] [PubMed]
15. Lü, J.; Chen, G. Generating multiscroll chaotic attractors: Theories, methods. *Int. J. Bifurc. Chaos* **2006**, *16*, 775–858. [CrossRef]
16. Yu, S.; Lü, J.; Chen, G. Theoretical design and circuit implementation of multidirectional multi-torus chaotic attractors. *IEEE Trans. Circuits Syst. I Regul. Pap.* **2007**, *54*, 2087–2098. [CrossRef]
17. Lü, J.; Murali, K.; Sinha, S.; Leung, H.; Aziz-Alaoui, M.A. Generating multi-scroll chaotic attractors by thresholding. *Phys. Lett. Sect. A Gen. Atomic Solid State Phys.* **2008**, *372*, 3234–3239. [CrossRef]
18. Xu, F.; Yu, P. Chaos control and chaos synchronization for multi-scroll chaotic attractors generated using hyperbolic functions. *J. Math. Anal. Appl.* **2010**, *362*, 252–274. [CrossRef]
19. Liu, C.; Yi, J.; Xi, X.; An, L.; Qian, Y.; Fu, Y. Research on the Multi-Scroll Chaos Generation Based on Jerk Mode. *Procedia Eng.* **2012**, *29*, 957–961.
20. Zuo, T.; Sun, K.; Ai, X.; Wang, H. High-order grid multiscroll chaotic attractors generated by the second-generation current conveyor circuit. *IEEE Trans. Circuits Syst. II Express Briefs* **2014**, *61*, 818–822. [CrossRef]
21. Choo, L.C.; Ling, C. Superposition lattice coding for Gaussian broadcast channel with confidential message. In Proceedings of the 2014 IEEE Information Theory Workshop, Hobart, TAS, Australia, 2–5 November 2014; pp. 311–315.
22. Yu, S.; Tang, W.K.S.; Lü, J.; Member, S.; Chen, G. Generation of $n \times$ m-Wing Lorenz-Like Attractors from a Modified Shimizu–Morioka Model. *IEEE Trans. Circ. Syst. II Express Briefs* **2008**, *55*, 1168–1172. [CrossRef]
23. Wang, F.-Q.; Liu, C.X. Generation of multi-scroll chaotic attractors via the saw-tooth function. *Int. J. Modern Phys. B* **2008**, *22*, 2399–2405. [CrossRef]
24. Lin, Y.; Wang, C.H.; Yin, J.W.; Hu, Y. A Simple Grid Multiscroll Chaotic Electronic Oscillator Employing CFOAs. *Int. J. Bifurc. Chaos* **2014**, *24*. [CrossRef]
25. Hu, X.; Liu, C.; Liu, L.; Yao, Y.; Zheng, G. Multi-scroll hidden attractors and multi-wing hidden attractors in a 5-dimensional memristive system. *Chin. Phys. B* **2017**, 26. [CrossRef]
26. Tahir, F.R.; Ali, R.S.; Pham, V.T.; Buscarino, A.; Frasca, M.; Fortuna, L. A novel 4D autonomous 2n-butterfly wing chaotic attractor. *Nonlinear Dyn.* **2016**, *85*, 2665–2671. [CrossRef]

27. Schultz, A.; Rekeczky, C.; Szatmari, I.; Roska, T.; Chua, L.O. Spatio-temporal CNN algorithm for object segmentation and object recognition. In Proceedings of the 1998 Fifth IEEE International Workshop on Cellular Neural Networks and Their Applications, London, UK, 14–17 April 1998; pp. 347–352.
28. Arena, P.; Baglio, S.; Fortuna, L.; Manganaro, G. Chua's Circuit Can Be generalized by CNN Cells. *IEEE Trans. Circuits Syst. I Fundam. Theory Appl.* **1995**, *42*, 123–125. [CrossRef]
29. Rahma, F.; Fortuna, L.; Frasca, M. New Attractors and New Behaviors in the Photo-Controlled Chua's Circuit. *Int. J. Bifurc. Chaos* **2009**, *19*, 329. [CrossRef]
30. Huang, X.; Zhao, Z.; Wang, Z.; Li, Y. Chaos and hyperchaos in fractional-order cellular neural networks. *Neurocomputing* **2012**, *94*, 13–21. [CrossRef]
31. Günay, E.; Altun, K. Multi-Scroll Chaotic Attractors in SC-CNN via Hyperbolic Tangent Function. *Symmetry* **2018**, *7*, 67. [CrossRef]
32. Günay, E.; Altun, K. Switched State Controlled-CNN: An Alternative Approach in Generating Complex Systems with Multivariable Nonlinearities Using CNN. *Int. J. Bifurc. Chaos* **2018**, *28*, 1830019. [CrossRef]
33. Arena, P.; Baglio, S.; Fortuna, L.; Manganaro, G. SC-CNN Based systems to realize a class of autonomous and coupled chaotic circuits. In Proceedings of the 1997 IEEE International Symposium on Circuits and Systems, Hong Kong, China, 9–12 June 1997.
34. Chua, L.O.; Yang, L. Cellular Neural Network: Theory. *IEEE Trans. Circ. Syst.* **1988**, *35*, 1257–1272. [CrossRef]
35. Chua, L.O.; Yang, L. Cellular Neural Networks: Applications. *IEEE Trans. Circuits Syst.* **1988**, *35*, 1273–1290. [CrossRef]
36. Chua, L.O.; Roska, T. *Cellular Neural Networks and Visual Computing: Foundations and Applications*; Cambridge University Press: Cambridge, England, 2002.
37. Deregel, P. Chua's Oscillator: Azoo of attractors. *J. Circuits Syst. Comput.* **1993**, *3*, 309–359. [CrossRef]
38. Kevorkian, P. Snapshots of Dynamical Evolution of Attractors from Chua's Oscillator. *IEEE Trans. Circ. Syst.* **1993**, *40*, 762–780. [CrossRef]